Influence of Different Strain Rates on the Flow Curve and the Formability of Thin Aluminium and Tinplate Sheets

M. Linnemann*, T. Lieber, C. Scheffler, V. Psyk, R. Müller, D. Landgrebe

Fraunhofer Institute for Machine Tools and Forming Technology (IWU), Chemnitz, Germany
*Corresponding author. E-mail: maik.linnemann@iwu.fraunhofer.de

Abstract

Due to this high number of produced units and the very thin sheet metals used for beverage cans, precise production processes with high production volumes are necessary. To save expenses, while optimising these processes, numerical simulation methods are exploited. Considering this, it is indispensable to identify the material behaviour as exactly as possible. In practise, often results of quasi static tensile tests are used, although these are insufficient for the precise modelling of the material behaviour during can production, since strain rates of up to 10^3 s^{-1} can occur, here. Therefore, quasi static and high speed tensile test have been done on specimens featuring the typical materials and thicknesses of semi-finished parts used for beverage can production. The results were compared with similar materials at higher sheet metal thicknesses and authenticated by numerical simulation. It was shown that there is an influence of the strain rate on the material behaviour and it is necessary to determine material characteristics at strain rates, which are close to the process speed. Furthermore, the results were classified in their signification for beverage can production and forming technologies in general.

Keywords

Material, Can manufacturing, High speed tensile test

1 Introduction

Economic and resource efficient manufacturing becomes more and more important in modern production technologies. This means, that e.g. in order to exploit the volume of the material used for component production as ideally as possible thickness should be preferably low. This plays an important role, especially for mass products as e.g. beverage cans. The number of produced beverage cans in the European Union increased from 45 billion pieces in 2006 to 63 billion pieces in 2014 (Statista GmbH, 2015). Due to this high number of units automated and very quick production processes with high forming speeds are necessary. Nowadays, up to 2000 cans per minute can be produced (Achhammer & Auburger, 2015).

To allow maximum material exploitation, highly accurate dimensions and shape, as well as good reproducibility of the semi-finished and finished products along the complete production chain are necessary. Therefore, the processes are designed by numerical methods. For this purpose, precise material properties are indispensable. In practise, the material properties are usually determined by quasi static tensile tests and strain rate sensitivity of the material behaviour is neglected. However, this is a simplifying approximation of the material behaviour only. Thus, it is not guaranteed to create exact results for high-speed production processes. This is why it is insufficient to represent the realistic behaviour via quasi static tensile test.

2 Beverage Can Production

Beverage cans are one of the most important packages for drinks, next to bottles and drink cartons. They appeared on market for the first time in the USA in the 1930's (Ball Europe, 2016). At that time, they looked like usual tin cans and had to be opened by a can-piercer. Until now a lot of developments and improvements have been done. Today beverage cans consist of two parts: the shaft and the cap. In the USA nearly all cans are made of aluminium, while in Germany 90% are made of tin plates (Weddige, 2001). This difference results from local conditions, since the USA has a big aluminium lobby, while Germany has a long steel production tradition. Typical initial thicknesses of the can body, which is formed by deep-drawing and wall ironing **(Figure 1)**, are in the range of 0.1-0.3 mm.

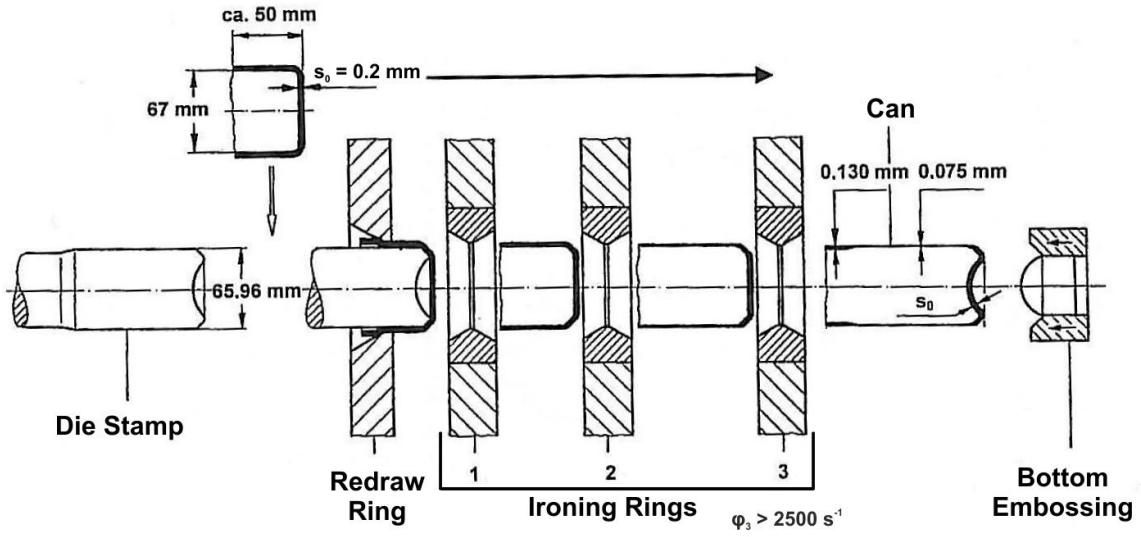

***Figure 1**: Forming Process adapted from Kaup (2003)*

In the production process of can body, small round blanks are formed cups by deep-drawing. Afterwards, these usually pass through 3 ironing rings to form the . Thereby, the wall thickness is reduced to 1/3 of the former thickness and the length increases accordingly. At the end, a die punch shapes the bottom of the can body. During these typical production processes, strain rates in the range of up to 10^3 s^{-1} can be achieved. (Kaup, 2003)

Nowadays, big efforts are made to optimise manufacturing processes in beverage can production. Main drivers are cost-reduction and an expansion of the market position. In the past, the optimisation was an expensive and time intensive experimental, but with numerical simulation it is more time efficient and related to lower costs, now. The numerical simulation allows designing a virtual model of the production process. Therefore, fundamental knowledge about process parameters and their interactions is necessary. Some of the most important parameters are the forming speed, the behaviour of the tools and the material characteristics of the raw material. With the developed numerical model it is easy to change parameters and check their influence on the production process without doing expensive changes in the real process. To achieve accurate results, this requires precise input data. In forming technologies especially a good material characterisation is needed. Therefore, it is indispensable to perform material test under realistic conditions.

3 Experimental Setup

3.1 Machine Properties and Test Conditions

All quasi static and high speed tensile tests regarded in this study were carried out at Fraunhofer IWU. For this purpose, two different Zwick/Roell testing machines were used. One machine is a ZPM 1475, which allows measuring a maximum force of 100 kN and operates with a maximum traverse speed of 1 m/min. It is used for quasi static tensile test at

a strain rate of 0.0003 s^{-1}, (according to) DIN EN ISO 6892-1 (2009). The elongation is measured by a clip-on extensometer.

For the high speed tests a HTM 16020 is used. It allows measuring a maximum force of 160 kN and operates with a maximum traverse speed of 20 m/s. The selected machine speed of 5 m/s results in a strain rate of 250 s^{-1} for the specimens regarded in this study. The elongation is measured by an optical extensometer. Therefore, black and white marks have to be placed on the specimen **(Figure 2)**.

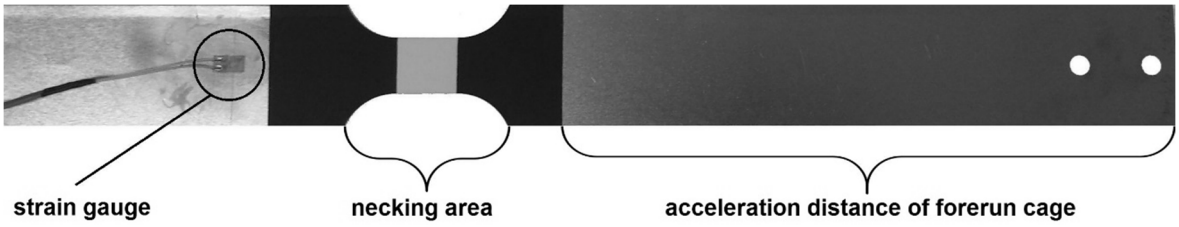

***Figure 2**: Specimen with black/white marks and strain gauge*

Due to the high strain rates, an oscillation, caused by the impact, superposes the measurement signal of the machine integrated load cell. That's why it is indispensable to apply strain gauges. Strain gauges have smaller mass compared to the load cell and can be attached close to the necking area.

3.2 Error Calculation

The experimental investigations with strain gauges are sensitive to parameter deviations. Besides of errors in the optical strain measurement, in particular the calculation of the force from the strain gauge can be erroneous. To investigate the impact of parameter deviations, an error calculation study was done (Taylor, 1988). The dependency of the force on the output voltage of the bridge circuit used for measuring the change of the resistance of the strain gauge is computed by **Eq. 1**:

$$F = \frac{E \cdot s_0 \cdot b \cdot U_0}{p \cdot k \cdot 100 \cdot U_B} \tag{1}$$

Here E is the Young's modulus, s_0 the sheet metal thickness, b the width of the specimen where the strain gauge is applied to, p a constant which is ½ for half bridges, k the strain gauge constant (2.0 for the applied strain gauge), U_o the measured output voltage and U_B the feeding voltage of the bridge network. Thus there are 5 relevant parameters x_i to be measured. The total differential can be applied to obtain an appropriate estimation of the error **(Eq. 2)**.

$$dF = \sum_{i=1}^{5} \frac{\partial F}{\partial x_i} dx_i \tag{2}$$

The absolute value of the partial derivation is a measure for the relative proportional impact on the total error, the so called participation factor. This factor must be still weighted

with the nominal value of the parameter itself to get the absolute share. The nominal values, used for calculating the participation factors, are E=210,000 N/mm^2, s_0=0.2 mm, b=44 mm, U_o=0.01 V (assumed for a strain of 1.10^{-3}) and U_B=10 V **(Eq. 3)**.

$$\left|E \cdot \frac{\partial F}{\partial E}\right| = \left|s_0 \cdot \frac{\partial F}{\partial s_0}\right| = \left|b \cdot \frac{\partial F}{\partial b}\right| = \left|U_o \cdot \frac{\partial F}{\partial U_0}\right| = \left|U_B \cdot \frac{\partial F}{\partial U_B}\right| = \frac{E \cdot s_0 \cdot b \cdot U_o}{p \cdot k \cdot 100 \cdot U_B} = 18.5 \quad (3)$$

It is obvious that all the parameters have the same impact on the error of the force because the value of the individual participation factors is equal. This is a result of the linear formula and the reason, why the same measurement accuracy should be taken into account for all parameters. This means, that for example the dimensions of the probe should be measured with the same high accuracy as the bridge voltages are measured and imposed.

4 Results and Discussion

Based on the force and displacement measurements, taken during the tensile tests, strain-stress-diagrams were created and used to determine the material characteristics yield strength $R_{p0,2}$, ultimate tensile strength R_m, and elongation at fracture A_{20} (see ***Table 1***.) and flow curves (see ***Figure 3***).

	material	**thickness [mm]**	**quasi static**			**high speed**		
			$R_{p0,2}$	R_m	A_{20}	$R_{p0,2}$	R_m	A_{20}
			in N/mm²		**in %**	**in N/mm²**		**in %**
1	EN AW-5182	0.35	346	411	8	337	395	19
	T52BA	0.16	252	317	38	415	435	38
	T52BA	0.20	227	304	40	407	433	40
2	EN AW-5182	1.20	150	300	30	160	275	35
	DC04	0.90	190	320	35	380	510	35

Table 1*: Material characteristics (1: beverage can materials, 2: comparative materials)*

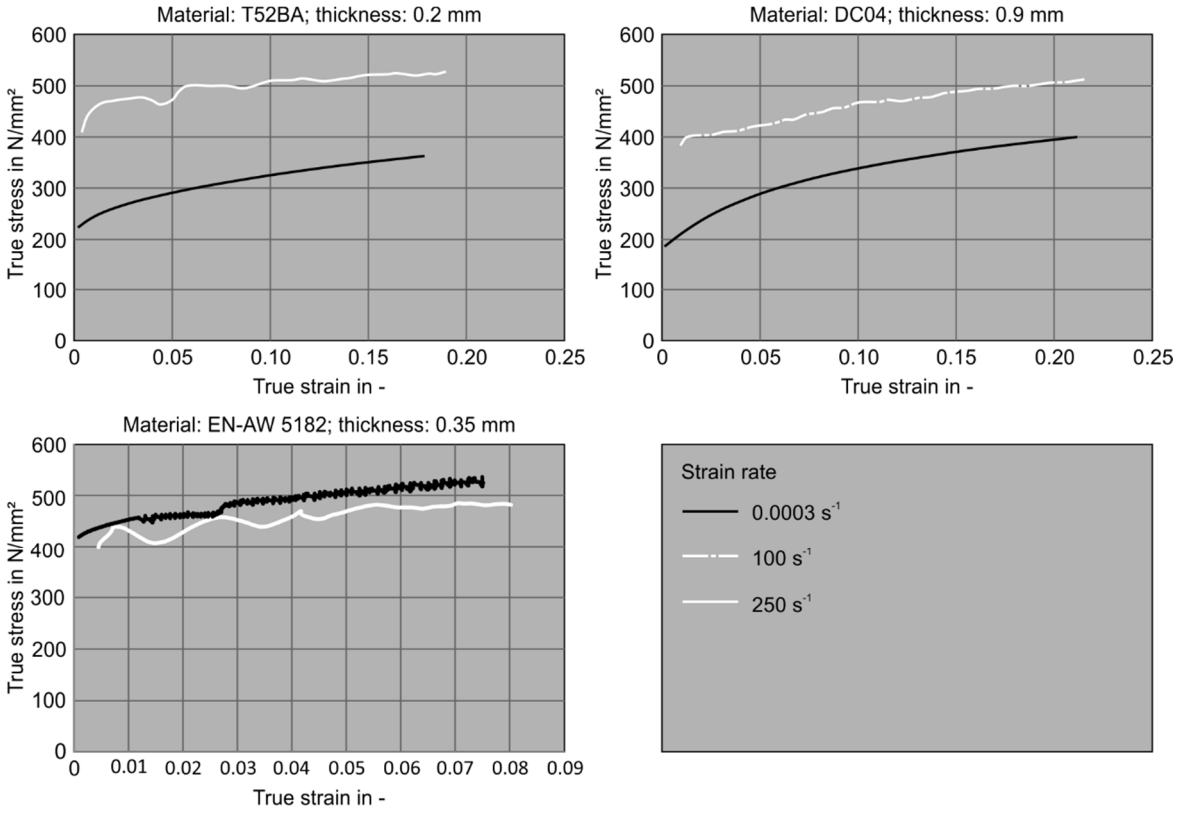

***Figure 3**: Flow curves (from onset of yielding to begin of necking)*

As expected, the measurement on the aluminium and the tin plates reveal significantly different results (see Table 1 and Figure 3). For the tin plates there is no influence of the strain rate on the elongation at fracture. However, there is a significant influence on yield strength and ultimate tensile strength. For both thicknesses of the tin plates the yield strength increases about 170 N/mm² and the ultimate tensile strength increases about 120 N/mm². Furthermore, the measurement results show that there is a difference in the yield strength and the ultimate tensile strength between the different sheet metal thicknesses for both strain rates, which can be explained as a consequence of the rolling process. The tin plate with 0.16 mm contains a stronger deformation and more significant strain hardening compared to the 0.20 mm tin plate.

DC04 - another unalloyed deep drawing steel – shows the same principle behaviour of yield stress and tensile strength for thicker sheets (0.9 mm), as shown in Figure 3 (top, right). DC04 is a low-alloyed steel, which is used for numerous forming applications. Consequently, its behaviour is well known and that is why older measurements performed at Fraunhofer IWU on this material are used as reference, here.

In case of aluminium specimens, the yield stress and the tensile strength at elevated strain rates in the range of 250 s^{-1} are about 10 N/mm² lower than in the quasi-static test (compare Table 1). This is in good agreement with the negative strain rate sensitivity of EN AW-5182 detected by Ostermann (2007). Accordingly, the influence of the strain rate on the material strength can be considered as minor compared to the regarded steel materials. However, there is a big influence on the elongation at fracture. The material characteristics

show that the elongation at fracture increases by nearly 240 % due to the increase in the strain rate (compare Table 1). Both effects are in good agreement with earlier investigations by Meyer et al. (2009).

Certainly, the increased forming limit of the aluminium at elevated strain rates is related to the so called Portevin–Le Chatelier (PLC) effect, which can be seen in the flow curve of EN AW-5182 (Figure 3, bottom, left). As Abbadi et. al (2002) figured out, the PLC effect is a plastic instability typical for aluminium alloys of the 5000 series. It occours if there are diffusing solute atoms within the lattice structure of the alloy. These are typically concentrated at the glide dislocation, because there most space is available. If the material is loaded with stress, the dislocations move along the slip planes. The diffusing solute atoms follow the dislocations and constrict their movement- the stress increases. After a critical stress the dislocation break away from the diffusing solute atoms and the stress suddenly collapses. Then, the process begins all over again. This effect can be seen as serrations in the stress-strain-diagram. If a critical strain rate is exceeded, it is impossible for the diffusing solute atoms to follow the dislocations. Accordingly, stress strain curves for higher strain rates typically do not feature the serration. The movement of dislocations is more homogeneous and thus the specimen can bear higher elongation at fracture. Measurements performed on specimens of the same aluminium alloy (EN AW- 5182) but featuring higher sheet thickness (1.2 mm) show similar effects (see Table 1).

5 Numerical Modelling

To enhance the understanding of the experimental results a numerical model for the high speed tensile test specimen with material T52BA 0.2 mm thickness and a velocity of 5 m/s was set up. Due to the short time duration of the experiment the Finite Element software LS-DYNA with its explicit solver was used. The model consists of about 90k full integrated shell elements and features for the specimen material a standard isotropic von Mises plasticity model enhanced by a nonlinear strain dependent damage and failure model (LSTC, 2015). This model (see **Figure 4**) accounts for the effect of damage prior to rupture based on an effective (equivalent) plastic-strain measure ε^{p}_{eff} without the consideration of the stress state. It is assumed that damage evolution begins at a strain $\varepsilon^{p}_{damage}= 0.3$ and ends with failure corresponding to the determined elongation at fracture with a damage variable D=1. The damage variable describes the relation of the void area A_{damage} to the total area A and scales the true stress σ_{damage}. The relative simplicity of the damage model proved its validity by a successful application for several sheet metal problems at the Fraunhofer IWU. The consideration of the strain rate scaling effect on the yield stress was considered by a strain rate table corresponding to the performed experiments with linear extrapolation beyond the tested strain rates. This was done in order to regard the much higher strain rates in the simulation of beverage can production. The simulation showed that the result of the material test with a strain rate of 250 s^{-1} can be seen as representative for higher strain rates.

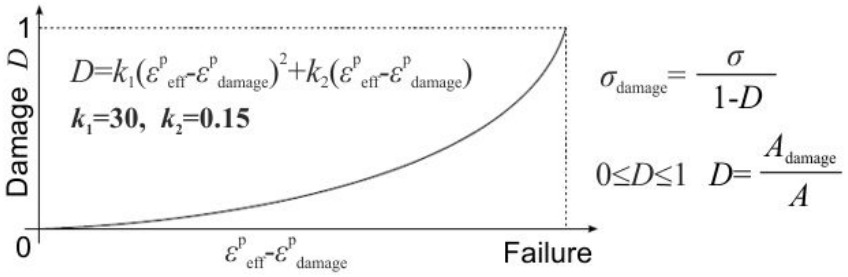

***Figure 4**: Damage evolution curve and model for material T52BA*

The results of the simulation for equivalent plastic strain and temperature are depicted in **Figure 5**. The figure shows a state just before failure occurs. The formation of the crack is triggered by the strain localisation in the specimen. The angle of the crack is 41° to the main axis of the specimen and is a result of the main shear stress. This failure mode is typical for a thin tensile test probe and is in good agreement with the experiment. However, the occurrence of the "arrow" shaped failure mode in Figure 5 is not the only valid mathematical solution for the crack problem. The inclined but straight crack propagation is valid as well and appears in about half of the experimental investigations. This means that from the mathematical fracture mechanics point of view the crack propagation has a bifurcation point in its solution.

It is well-known that the element size in simulations has a significant impact at the failure due to an insufficiently discretised strain field in the localisation zone (Feucht, 2011). To investigate the element size dependency of the failure behaviour, two mesh sizes, one with 50 µm element length in the relevant specimen zone and the other one with 100 µm length were investigated to determine local strains and strain rates. Figure 5 reveals that the global plastic strain in the specimen, determined as average over the parallel section, is at the time of crack initiation around 0.207, whereas the local strains are up to 0.46 for the 50 µm mesh size model and 0.43 for the 100 µm mesh model in the localization zone. The insignificant differences in the local strains indicate that the characteristic length scale of the material is almost achieved by the size of the spatial discretisation. The same can be identified for the strain rate distribution in the specimen where the global strain rate in the specimen is at 5 m/s test velocity 250 s^{-1} whereas the local strain rate in the localization zone can reach values of up to 25,000- 40,000 s^{-1} and even before localisation appears the maximum values are in the range of 500- 650 s^{-1}, see **Figure 6**. This figure shows the evolving shear bands, which finally grow together and intensify up to the crack initiation. Shear bands are also slightly visible in the experimental specimen (Figure 5, right).

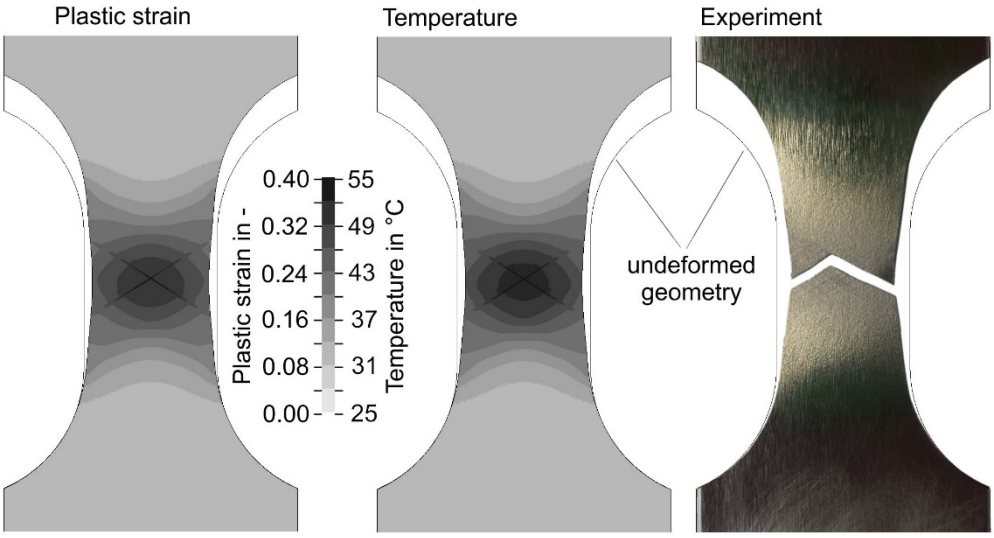

***Figure 5**: Plastic strain and temperature distribution right before crack propagation*

The increase in strain and temperature before rupture is obvious and a result of the localisation. Nevertheless the temperature increase is less than expected. This might be a result of the moderate test velocity of 5 m/s. The average temperature in the middle of the specimen area, where the maximum strain occur, is around 49°C, whereas in the localisation zone around 57°C occur (50 µm mesh size model). The boundary conditions for the coupled thermo-mechanical computation had been assumed as adiabatic. The time history evaluation of a point in the localisation zone is depicted in Figure 6.

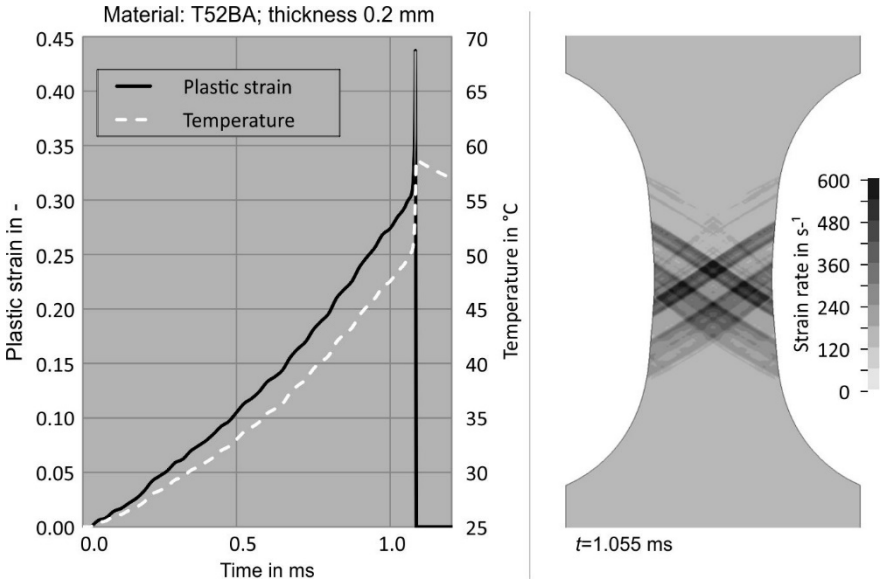

***Figure 6:** Left: plastic strain and temperature evolution for a point in the localisation zone. Right: Strain rate distribution with distinct shear bands before failure.*

6 Conclusion

In order to provide fundamental knowledge on the material behaviour of thin sheet metals for the numerical simulation of beverage can production processes, quasi static and high speed tensile tests were carried out. Two different strain rates (0.0003 s^{-1}, 250 s^{-1}) and two materials relevant for can production (tin plates with thicknesses of 0.2 mm and 0.16 mm and aluminium with a thickness of 0.35 mm) were chosen. The results show that there are severe differences in the behaviour of tin plates and aluminium. However, for both materials the tests have shown that quasi static tensile tests alone are insufficient to describe the material characteristics at higher strain rates, which are definitely relevant for can production. Thus, it is essential to determine the material characteristics for the full range of strain rates occurring during beverage can production in order to create realistic and reliable numerical models.

A look at the T52BA tin plates reveals that for this material at elevated strain rates the yield stress and the tensile strength are higher, resulting in higher forming forces. Consequences for the process design are that bigger machines, which can provide the higher forces, are required and more energy is needed to run them. In addition to this, higher wear of the tool can lead to higher costs for tool maintenance and repair, respectively. On the other hand, there is no measurable influence of the strain rate on the elongation at fracture for the regarded range of strain rates in case of the steel material. Thus, no deterioration of the formability related to the strain rate has to be taken into consideration, when dimensioning the product and the production steps.

The results of the EN AW-5182 show a more favourable behaviour from the point of view of forming technologies. For this material, no increase of the material strength was detected at higher strain rates and within the range of strain rates regarded in this study, even a slight decrease in the strength can be recognised for higher strain rates. This means that the above mentioned disadvantages related to the higher forming forces are not relevant, here. At the same time, the formability, characterised via the strain at failure, significantly increases at higher strain rates, which directly leads to a remarkable increase of the forming limits. Detailed knowledge about this will allow extending the design freedom in can production and enable completely new shapes and details. This general trend also suggests that the use of high speed forming techniques as electromagnetic forming, during which even higher strain rates of up to 104 s^{-1} are reached (Psyk et al., 2011), is predestined for fully exploiting this potential.

References

Abbadi, M., Hähner, P., & Zeghloul, A. (2002). On the characteristics of Portevin–Le Chatelier bands in aluminum alloy 5182 under stress-controlled and strain-controlled tensile testing. Materials Science and Engineering(A337), pp. 194 - 201.

Achhammer, K.-H., & Auburger, M. (2015, February 25th). Patent No. EP2838834 A1.

Ball Europe. (2016). Retrieved 01 2016, 14, from http://www.ball-europe.com/businesscards/de/911.htm

Feucht, M.; Neukamm, F.; Haufe, A. (2011). A Phenomenological Damage Model to Predict Material Failure in Crashworthiness Applications. In: Recent Developments and Innovative Applications in Comp. mechanics, Müller-Höppe, et al., Springer Berlin Heidelberg.

DIN EN ISO 6892-1. (2009). Metallische Werkstoffe - Zugversuch - Teil 1: Prüfverfahren bei Raumtemperatur. 81. Berlin: Beuth Verlag.

Kaup, B. (2003). Optimierung der Umform- und Gebrauchseigenschaften von tief entkohltem Stahl zur Fertigung von zweiteiligen Getränkedosen. Aachen: Shaker Verlag.

LSTC (2015). LS-DYNA Keyword User's Manual. Volume II. Livermore Software Technology Corporation (LSTC)

Meyer, L. W., Herzig, N., Halle, T., & Abdel-Malek, S. (2009, March 12th). Werkstoffverhalten bei hohen Dehnungsgeschwindigkeiten. Workshop Impulsumformung.

Psyk, V., Risch, D., Kinsey, B. L., Tekkaya, A. E., & Kleiner, M. (2011). Electromagnetic Forming - A Review. Journal of Materials Processing Technology (211), pp. 787 - 829.

Statista GmbH. (2015, September). Absatz von Getränkedosen in Europa nach Bereichen bis 2014 | Statistik. Retrieved 11 02, 2015, from http://de.statista.com/statistik/daten/studie/215739/umfrage/anzahl-der-getraenkedosen-von-bier-und-alkoholfreien-getraenken-in-europa/

Taylor, J. R. (1988). Fehleranalyse. VCH Verlagsgesellschaft, Weinheim-Basel-Cambridge-New York.

Weddige, H.-J. (2001). Stahl im Wettbewerb der Werkstoffe. Freiberg.